

accepted that solar flares are driven by magnetic reconfiguration, suggesting that the evolution of the magnetic field in the interior of the Sun may have clear and visible consequences in the solar atmosphere. These effects can be seen at different heights, revealing important physical processes related to the dynamics of the flare itself. In the chromosphere and photosphere, flares are seen as sudden brightness increases in the hydrogen absorption lines. In some instances there is excess visible-continua emission, in what is called the “white-light flare” phenomenon.

The first solar flare was discovered by Carrington (1859) by its excess emission of white light. The intensity of excess white light in some flares represents the release of considerable energy in the lower atmosphere in a few seconds or minutes. In the upper atmosphere and corona, X-ray signatures indicate the existence of electrons accelerated to tens of keV. In some flares, γ -rays may also appear, and these reveal the presence of protons with energies in excess of some 10 MeV. In white-light flares, the onset of the continuum emission is in the impulsive phase. Its source is deep in the solar atmosphere, extending into the near-IR spectrum, including even the “opacity minimum” at $\approx 1.5 \mu\text{m}$ (Xu *et al.*, 2004). In spite of the photospheric origin of most of this part of the spectrum in non-flaring conditions, strong evidence implicates the chromosphere for at least part of the excess in white-light flares. The continuum emission has signatures of recombination radiation (Neidig, 1986; Hudson, Fletcher, and Krucker, 2010). Moreover, the source of the visible continuum appears to correlate well with hard X-rays (Švestka, 1970; Rust and Hegwer, 1975; Hudson *et al.*, 1992; Martínez Oliveros *et al.*, 2012). The *Helioseismic and Magnetic Imager* (HMI) onboard the *Solar Dynamics Observatory* (SDO) gives us a new opportunity to study the white-light enhancement produced by flares and explore the close relation it has with the energy deposition observed in hard X- and γ -rays. This is possible because of the spatial and spectral capabilities of HMI (Schou *et al.*, 2012). The HMI data clearly resolve the profile of the Fe I line at 6173.34 \AA , in each $\approx 0.5''$ pixel and 45-second time step.

The present study recognizes such an instance in a study by Martínez Oliveros *et al.* (2011), herein Paper I, of the highly impulsive M2.2-class flare of SOL2010-06-12T00:57. During the impulsive phase of this flare, a bright white-light kernel appeared in each of the two magnetic footpoints revealed by hard X-ray emission. When the flare occurred, the spectral coverage of the HMI filtergrams (six equidistant samples spanning $\pm 172 \text{ m\AA}$ around nominal line center) encompassed the line core and the blue continuum sufficiently far from the core to eliminate significant Doppler crosstalk in the latter, which is otherwise a possibility for the extreme conditions in a white-light flare. The Fe I line appears to be shifted to the blue during the flare but does not go into emission; the contrast is nearly constant across the line profile.

In this study, then, we show that Doppler signatures in SDO/HMI observations of white-light flares, while excellent in many other respects, are subject to strong artifacts, because different parts of the spectrum are recorded at different times, between which the respective intensities undergo significant variations. The instruments used by the *Global Oscillations Network Group* (GONG) are essentially free of these artifacts, because all parts of the spectrum are effectively

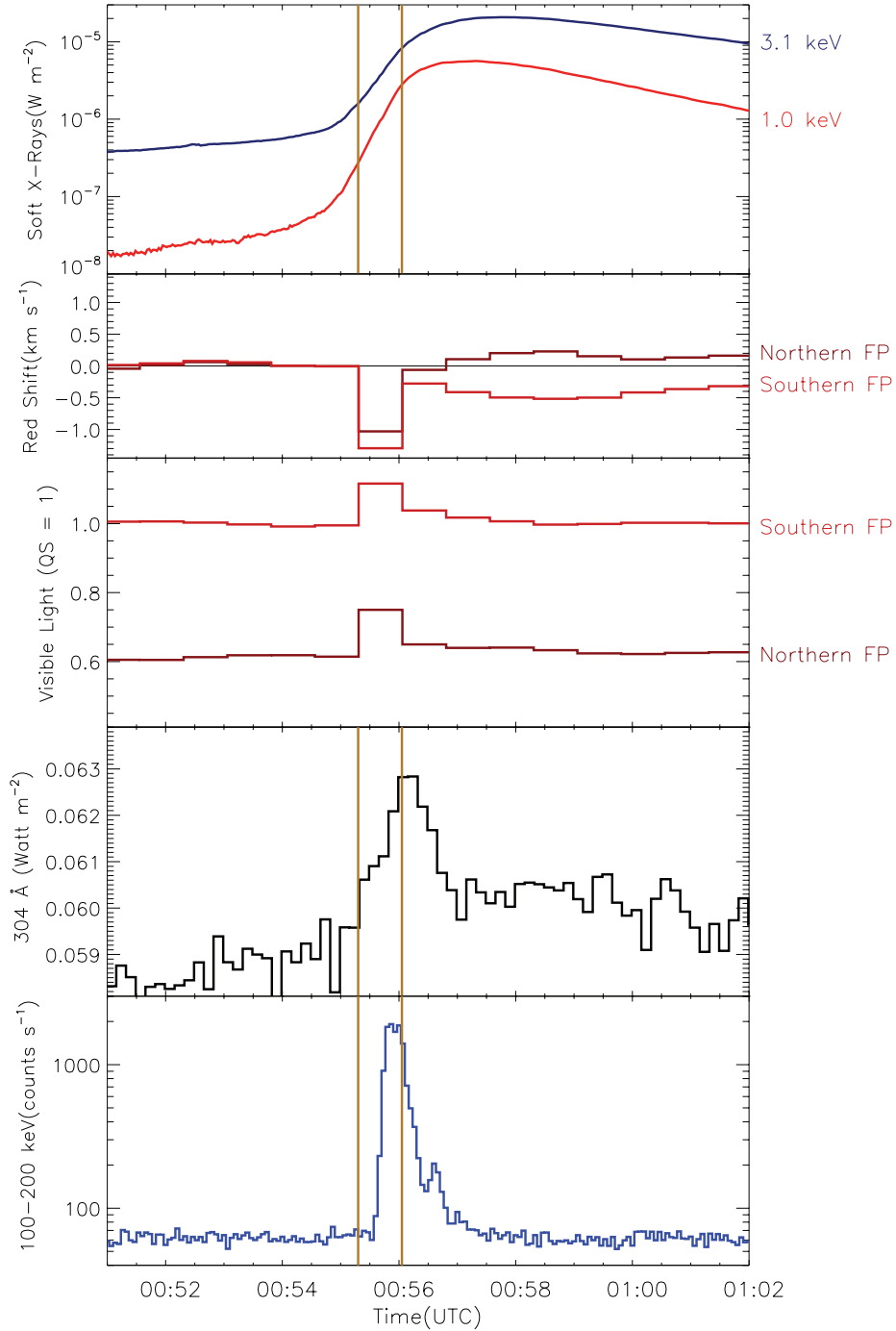


Figure 1. Overview of the temporal development of SOL2010-06-12T00:57. The five panels show (top to bottom): GOES soft X-rays, HMI NRT (“near real time”) redshifts in the two flaring footpoints, continuum brightnesses in the two regions, EVE 304 Å excess irradiance, and RHESSI (Lin *et al.*, 2002) 100–200 keV hard X-ray flux. The vertical lines show the beginning and end of the sampling interval of the HMI observations used to construct the Doppler signature (see also Table 1). Reproduced by permission from Martínez Oliveros *et al.* (2011).

measured at the same time. Even so, this does not imply that the GONG++¹ observations are correct or impervious to other kinds of artifacts, as demonstrated by Maurya and Ambastha (2010). We should mention that artifacts in HMI data have been reported before (*e.g.* Maurya, Vemareddy, and Ambastha, 2012), but, the nature of these artifacts we believe to be different, and to have similar properties to those reported by Qiu *et al.* (2002) and Qiu and Gary (2003).

The major disadvantage of the GONG++ observations is the smearing of the images due to atmospheric turbulence. This limits spatial resolution. However, more troubling, variations in this smearing from one image to the next introduces strong artifacts in features that have strong spatial intensity gradients, such as active regions. We have developed a “Parametric Smearing Correction ALgorithm” (PASCAL) to correct these artifacts (Lindsey and Donea, 2008) and applied it to GONG++ observations of SOL2010-06-12T00:57 for comparison with the SDO/HMI Doppler signatures. The GONG++ Doppler observations, while highly consistent with the HMI Doppler observations in non-flaring conditions, show no facsimile of the strong blueshift indicated by the HMI Doppler observations in the impulsive-phase foot points of the flare. On the contrary, they rather show a weak redshift at those locations at that time (see Section 3). Figure 1 compares the HMI Doppler and intensity signatures temporally with UV and X-ray observations from *Geostationary Operational Environmental Satellite* (GOES), *Reuven Ramaty High Energy Solar Spectroscopic Imager* (RHESSI) and *Extreme ultraviolet Variability Experiment* (EVE).

2. The PArametric Smearing Correction ALgorithm (PASCAL)

The GONG++ network provides us high-quality Doppler and white-light observations of the Sun. The significant limitation of these data for active-region observations is the smearing of the solar image due to atmospheric turbulence. This imposes familiar limits on spatial resolution. For active-region seismology, the main liability of image smearing is noise in the helioseismic signature due to variations in the amount of smearing from one image to the next. In the quiet Sun, these variations are small compared to the signatures that GONG++ is designed to image. However, the effect of temporal variations in the smearing acting on the large intensity gradients intrinsic to sunspots, for example, introduce noise that competes with helioseismic signatures. Until recently, this has made seismology of active regions from GONG++ data impractical except under unusually good atmospheric conditions (Toner and Labonte, 1993).

Lindsey and Donea (2008) devised an algorithm that discriminates most of this noise from helioseismic signals, making active-region seismology based on GONG++ observations practical on terms similar to that for the quiet Sun in moderately good atmospheric conditions. The method is specifically applicable to observations that are integrated over a time that is long, one minute for the GONG++ observations, compared to the characteristic time for atmospheric

¹GONG++ is an upgrade of the GONG 256x256 to 1024x1024 pixel cameras (known as GONG+, Harvey, Tucker, and Britanik, 1998) and its corresponding data processing system.

turbulence in the telescope beam, typically ≈ 30 ms, with high tracking accuracy based on location of the solar limb. Under these conditions, the resulting smearing is highly isotropic in the image plane. The noise that competes with seismic observations in an active region is the result of differential variations in the degree of smearing from one integration to the next. The method that Lindsey and Donea (2008) developed applies a measured “adjustment” in smearing to each GONG++ image to devise a resultant smear that is effectively the same for all images. The method is greatly simplified by the recognition that the difference between two images can be well represented by a constant times the Laplacian of the average of the two images. Lindsey and Donea (2008) describe the method analytically, applying it successfully to GONG++ intensity observations of the white-light flare SOL2003-10-29.

Lindsey and Donea (2008) successfully applied the technique to GONG++ continuum images. More recently its extension to Doppler helioseismic applications has been demonstrated by Zharkov, Zharkova, and Matthews (2011). Because GONG++ Doppler and magnetic images are linear combinations of intensity maps in different wavelengths and polarizations, and the Laplacian is a linear operator, the extension of the technique to GONG++ Doppler and magnetic images is straightforward.

For a given time series of n GONG++ intensity images, indexed by $i \in \{1, 2, 3, \dots, n\}$, this entails first deriving a set σ_i of smearing parameters that characterizes each respective intensity image. The smearing of each intensity, Doppler, and magnetic image is then adjusted differentially to eliminate stochastic variations in σ_i from one to the next. It is important to understand that the foregoing procedure will not substantially recover high spatial resolution lost as a result of atmospheric turbulence. It only eliminates spurious intensity variations due to differential variations in the amount of smearing. This procedure will make it possible to apply the same helioseismic techniques to active regions in GONG++ observations as in the concurrent space-borne *Michelson Doppler Imager* (MDI) observations. This includes the large inventory of acoustically active flares that MDI onboard the *Solar and Heliospheric Observatory* (SOHO) will have to have missed because of limited ($\sim 20\%$) temporal coverage of Cycle 23 after the advent of GONG++, as well as the SDO/HMI events.

3. Observations and Analysis

In Paper I we studied the M2.0-class flare SOL2010-06-12T00:57 (NOAA 11081, located approximately at N22W45). This flare had a remarkably impulsive hard X-ray light curve, with a duration (half maximum at 50 keV) of only about 25 seconds. It also produced γ -ray emission, unusual for such a weak event (Shih, Lin, and Smith, 2009). Figure 1 compares time series representing HMI intensity and Doppler observations with soft (GOES) and hard (RHESSI) X-ray fluxes. Table 1 summarizes these phenomena seen in the relevant HMI intervals and gives them names, “Preflare,” “Brightening,” and “Postflare,” for subsequent reference. The hard X-ray signature mainly matches the Brightening interval (the white-light flare) and does not extend earlier into the previous HMI integration.

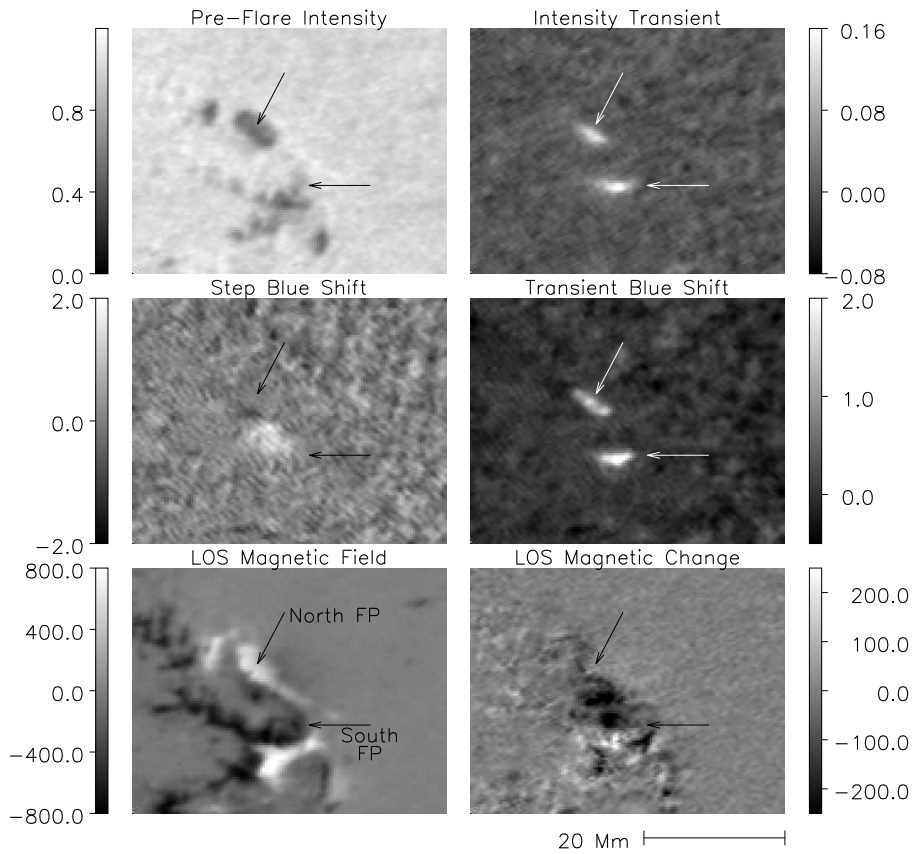


Figure 2. HMI “near real time” (NRT) images: top-left, HMI preflare continuum image; top-right, transient continuum excess over the preflare continuum; middle-left, Doppler difference between pre- and post-flare intervals, showing a stepwise change in line-of-sight flow; middle right, map of blueshift in the impulsive phase minus the same 45 s earlier; lower left, the preflare line-of-sight magnetic field; and lower-right, the Postflare line-of-sight magnetic field minus the preflare line-of-sight field (see Table 1 for times). The arrows locate the footpoint sources. The grayscale shows fractions of quiet-Sun intensity, $[\text{km s}^{-1}]$, and Gauss for the top, middle and bottom rows, respectively.

Figure 2 shows maps of continuum, Doppler and line-of-sight magnetic signatures of the flare. The top-left frame shows the Preflare continuum intensity; the top-right frame shows the continuum excess during the Brightening phase; the middle-left frame shows the Doppler variation from Preflare to Postflare. The middle-right frame shows the same for Preflare to Brightening, the bottom left frame shows the Preflare line-of-sight magnetic field; the bottom-right frame shows its variation from Preflare to Postflare. Paper I noted strong Doppler-blueshift transients in both footpoints (middle-right frame of Figure 2). Time-series of these signatures are plotted in Figure 3. In Paper I the validity of this blueshift in the HMI Dopplergrams was questioned, but left the question

Table 1. Flare timeline in HMI data (45-second data frames)

Interval name	Start [UTC]	HMI continuum	HMI Doppler	RHESSI 100 keV
Preflare	00:54:11	no excess	no anomaly	none
Brightening	00:55:41	>10% increase	2 km s ⁻¹ blue	bright
Postflare	01:00:11	no excess	complex	no detection

unresolved. Such a blueshift, if real, could open significant issues to flare physics. Among the possible implications are rapidly up-flowing photospheric gas with the line in absorption; rapidly down-flowing chromospheric gas with the line from the chromospheric contribution in emission (but the composite line still in absorption); and rapid horizontal flows, noting that the line of sight at the foot points was inclined $\approx 50^\circ$ from vertical. The significant concern is that the intensity maps sampling different wavelengths are observed at different times. If the respective intensities change considerably in the respective interval, this will introduce a spurious Doppler signature even if there is never any spectral shift at any single moment during the sampling interval.

The most practical control for the validity of the Doppler transient seems to be by comparing the results of the analysis with other instruments. Hudson *et al.* (2011) show that for this event the EVE observations report a redshift of 16.8 ± 5.9 km s⁻¹ in the He II 304-Å line. This might possibly suggest that the blue Doppler transient is an artifact, but the gas represented by this line is in the transition region, the line being in emission rather than absorption. Indeed, a layer of down-flowing gas in the chromosphere or upper photosphere that by itself would appear in emission would manifest a *blue* shift if the composite line remained in absorption. So, this is not a practical control for the photospheric Doppler signatures.

What is needed is a comparison of the HMI observations with observations from an instrument that observes a photospheric line similar to that observed by HMI, but that samples all parts of the spectrum simultaneously. The GONG++ network provides such an instrument. Each instrument in the network is a Michelson Doppler tachometer that measures the spectral shift of the photospheric line Ni I 6768 Å, with an integration time of 60 seconds (Brown, 1984; Harvey *et al.*, 1996; Leibacher and GONG Project Team, 1995; Harvey *et al.*, 1996). SDO/HMI observes the slightly weaker line, Fe I 6173.34 Å with a 45-second cadence. This line features greater magnetic sensitivity, with the caution (Norton *et al.*, 2006) that this reduces the dynamic range over which HMI can reliably measure Zeeman splitting, given the limited spectral range sampled by the instrument and the considerable part of this range covered by solar rotation and motion of the spacecraft even without magnetic splitting.

The heights at which these lines form are significantly different, but the contribution functions overlap strongly. Fleck, Couvidat, and Straus (2011) studied the formation heights of the Fe I 6173-Å (HMI) and Ni I 6768-Å (MDI, GONG++) lines based on 3D radiation-hydrodynamic simulations. They found that the Fe I 6173-Å line is formed at a height ≈ 100 km, while the Ni I 6768-Å

line is formed at ≈ 150 km. Also, they studied the dependency of the height of formation on the spatial resolution, finding a small dependence that increases the height by about 40–50 km for HMI and 15–25 km for MDI. As a result the formation height of HMI Fe I 6173-Å and MDI Ni I 6768-Å lines become 140-150 km and 165–175 km, respectively. (For more details see Fleck, Couvidat, and Straus, 2011 and references therein).

A significant consideration in a comparison between GONG++ and HMI is the disparity in spatial resolution. SDO/HMI has far better spatial resolution than GONG++. In order to compare the footpoints in each instrument, the HMI images were rebinned to the GONG++ resolution, so that we could do the same analysis for both data sets. We applied the PASCAL algorithm to the GONG++ observations to correct for variable smearing by the Earth’s atmosphere. We then calculated the intensities and Doppler signatures averaged spatially over masks that encompassed the respective foot points in both GONG++ and HMI images. Because of the poorer spatial resolution in the GONG++ observations, the masks applied in this analysis were more extended than those applied in Paper I. The assumption at this moment is that if the HMI blueshift is valid, it should be clearly seen in the GONG++ Doppler time series. Figure 3 shows the intensity and velocity time series for both instruments. Both instruments show similar behaviors in the intensity data. Moreover, there is a strong correlation between the respective Doppler time series before and after the impulsive phase of the flare. The strong blueshifts reported in Paper I in the impulsive phase of the flare (vertical dashed line), although weaker when averaged over the more extended masks, remain clear in both of HMI Doppler time series. However, these features do not appear in the GONG++ Doppler time series. This points to the presence of a strong artifact in the HMI Dopplergrams when applied to transient phenomena such as those that occur in flares. We note again, that these results do not demonstrate the reliability of GONG++ data during flares, and only shows that the observed Doppler transient is an artifact in the HMI Dopplergrams.

4. Conclusions

We find that SDO/HMI Doppler observations, while excellent for nominal helioseismic applications, are subject to strong artifacts when applied to transient phenomena, such as occur in flares, as anticipated. This appears to be the result of rapid changes of the spectrum between the respective times at which different parts of it are being sampled. Because the GONG++ instrument effectively samples all parts of the spectrum simultaneously, it appears to be immune to Doppler artifacts of this kind, notwithstanding that both GONG++ and HMI remain subject to effects due to various aspects of radiative transfer in the flare environment and independent of considerations of relative timing. Similar considerations ought to apply to magnetograms, both line-of-sight and Stokes, during the impulsive phases of flares as determined by Maurya and Ambastha (2010). We know of no reason that these artifacts should be of any significant concern for

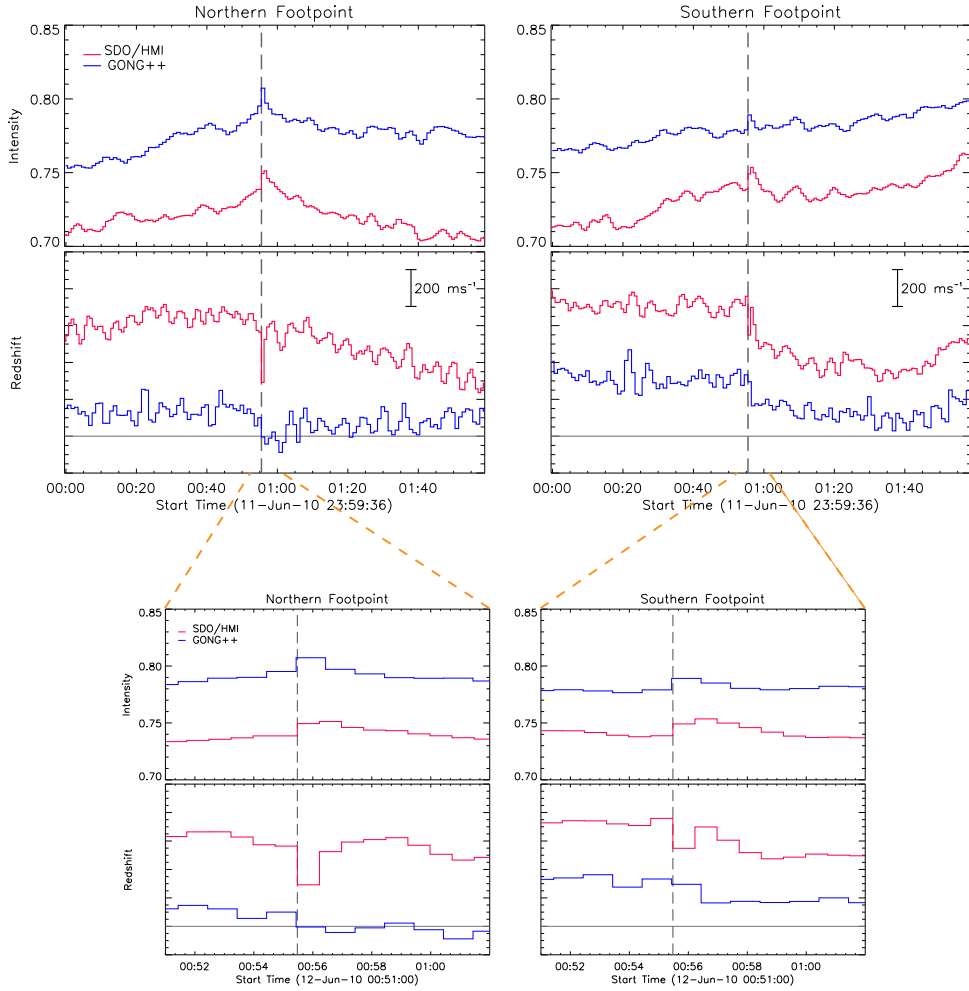


Figure 3. Comparison of GONG++ and HMI observations of SOL2010-06-12, isolating the two flare footpoints as resolvable by GONG++. Upper: intensity contrast relative to a quiet-Sun reference; lower: redshift. SDO/HMI data are in red, GONG++ in blue. The striking blue-shifted Doppler artifact seen by HMI in the impulsive phase (dashed vertical line) is absent in the GONG++ Doppler signatures. Note the strong correlations between the GONG++ and HMI time series in the intensity and Doppler time series other than in the Doppler time series during the impulsive phase. The bottom four frames show a closeup at the time of the artifact.

non-flaring applications of GONG++ or HMI observations, such as standard p -mode analysis (*e.g.* Basu *et al.*, 2003; Rajaguru, Hughes, and Thompson, 2004; Barban and Hill, 2004; Hughes, Rajaguru, and Thompson, 2005; Moradi *et al.*, 2007; Zharkov, Zharkova, and Matthews, 2011).

That GONG++ has been working for a little over a decade and half, and it has been possible to improve and refine its methods for obtaining and analyzing

helioseismic observations, reinforces its reliability for the range of applications to which it has been applied, which now include white-light flares along with the nominal helioseismic applications. The major disadvantage of GONG++ as a complement to SDO/HMI for transient phenomena is its poorer spatial resolution. Drifts in atmospheric smearing have made active-region seismology impractical until recently, with the development of the PASCAL algorithm. The application of PASCAL to GONG++ intensity observations has made it useful for the recognition and analysis of white-light flares (Lindsey and Donea, 2008; Paper I; this study). More recent applications to GONG++ Doppler observations by Zharkov, Zharkova, and Matthews (2011) have now established its utility for active-region seismology. These results argue in favor of a strong role for GONG++ as a complement to SDO/HMI in the rapidly developing field of flare seismology.

Acknowledgments: We thank Jesper Schou and Sebastien Couvidat for their valuable comments during the writing of this article. The Berkeley group was supported by NASA under contract NNX11AP05G, and the SDO/HMI by contract NAS5-02139 to Stanford University. These data have been used courtesy of NASA/SDO and the EVE and HMI science teams. This work utilizes data obtained by the Global Oscillation Network Group (GONG) Program, managed by the National Solar Observatory, which is operated by AURA, Inc. under a cooperative agreement with the National Science Foundation.

References

- Barban, C., Hill, F.: 2004, Comparison of GONG and MDI solar p-mode background. *Solar Phys.* **220**, 399–402. doi:10.1023/B:SOLA.0000031393.36840.7c.
- Basu, S., Christensen-Dalsgaard, J., Howe, R., Schou, J., Thompson, M.J., Hill, F., Komm, R.: 2003, A Comparison of Solar p-Mode Parameters from MDI and GONG: Mode Frequencies and Structure Inversions. *Astrophys. J.* **591**, 432–445. doi:10.1086/375331.
- Brown, T.M.: 1984, The Fourier tachometer 2: an instrument for measuring global solar velocity fields. In: Ulrich, R.K., Harvey, J., Rhodes, E.J. Jr., Toomre, J. (eds.) *Solar Seismology from Space*, NASA, JPL Publ. 157–163.
- Carrington, R.C.: 1859, Description of a Singular Appearance seen in the Sun on September 1, 1859. *Mon. Not. Roy. Astron. Soc.* **20**, 13–16.
- Fleck, B., Couvidat, S., Straus, T.: 2011, On the Formation Height of the SDO/HMI Fe 6173 Å Doppler Signal. *Solar Phys.* **271**, 27–40. doi:10.1007/s11207-011-9783-9.
- Harvey, J.W., Hill, F., Hubbard, R.P., Kennedy, J.R., Leibacher, J.W., Pintar, J.A., Gilman, P.A., Noyes, R.W., Title, A.M., Toomre, J., Ulrich, R.K., Bhatnagar, A., Kennewell, J.A., Marquette, W., Patron, J., Saa, O., Yasukawa, E.: 1996, The Global Oscillation Network Group (GONG) Project. *Science* **272**, 1284–1286. doi:10.1126/science.272.5266.1284.
- Harvey, J., Tucker, R., Britanik, L.: 1998, Structure and Dynamics of the Interior of the Sun and Sun-like Stars. In: Korzennik, S.G., Wilson, A. (eds.) *ESA SP-418*, ESA Publications Division, Noordwijk, The Netherlands 209.
- Hudson, H.S., Fletcher, L., Krucker, S.: 2010, The white-light continuum in the impulsive phase of a solar flare. *Mem. Soc. Astron. Italiana* **81**, 637.
- Hudson, H.S., Acton, L.W., Hirayama, T., Uchida, Y.: 1992, White-light flares observed by Yohkoh. *Pub. Astron. Soc. Japan* **44**, L77–L81.
- Hudson, H.S., Woods, T.N., Chamberlin, P.C., Fletcher, L., Del Zanna, G., Didkovsky, L., Labrosse, N., Graham, D.: 2011, The EVE Doppler Sensitivity and Flare Observations. *Solar Phys.* **273**, 69–80. doi:10.1007/s11207-011-9862-y.

- Hughes, S.J., Rajaguru, S.P., Thompson, M.J.: 2005, Comparison of GONG and MDI: Sound-Speed Anomalies beneath Two Active Regions. *Astrophys. J.* **627**, 1040–1048. doi:10.1086/430394.
- Leibacher, J., GONG Project Team: 1995, The Global Oscillation Network Group Project. In: Ulrich, R.K., Rhodes, E.J. Jr., Dappen, W. (eds.) *GONG 1994. Helio- and Astro-Seismology from the Earth and Space*, **76**, Conf. Ser. Astronom. Soc. Pac. 381.
- Lin, R.P., Dennis, B.R., Hurford, G.J., Smith, D.M., Zehnder, A., Harvey, P.R., Curtis, D.W., Pankow, D., Turin, P., Bester, M., Csillaghy, A., Lewis, M., Madden, N., van Beek, H.F., Appleby, M., Raudorf, T., McTiernan, J., Ramaty, R., Schmahl, E., Schwartz, R., Krucker, S., Abiad, R., Quinn, T., Berg, P., Hashii, M., Sterling, R., Jackson, R., Pratt, R., Campbell, R.D., Malone, D., Landis, D., Barrington-Leigh, C.P., Slassi-Sennou, S., Cork, C., Clark, D., Amato, D., Orwig, L., Boyle, R., Banks, I.S., Shirey, K., Tolbert, A.K., Zarro, D., Snow, F., Thomsen, K., Henneck, R., Mchedlishvili, A., Ming, P., Fivian, M., Jordan, J., Wanner, R., Crubb, J., Preble, J., Matranga, M., Benz, A., Hudson, H., Canfield, R.C., Holman, G.D., Crannell, C., Kosugi, T., Emslie, A.G., Vilmer, N., Brown, J.C., Johns-Krull, C., Aschwanden, M., Metcalf, T., Conway, A.: 2002, The Reuven Ramaty High-Energy Solar Spectroscopic Imager (RHESSI). *Solar Phys.* **210**, 3–32. doi:10.1023/A:1022428818870.
- Lindsey, C., Donea, A.: 2008, Mechanics of Seismic Emission from Solar Flares. *Solar Phys.* **251**, 627–639. doi:10.1007/s11207-008-9140-9.
- Martínez Oliveros, J.C., Couvidat, S., Schou, J., Krucker, S., Lindsey, C., Hudson, H.S., Scherrer, P.: 2011, Imaging Spectroscopy of a White-Light Solar Flare. *Solar Phys.* **269**, 269–281. doi:10.1007/s11207-010-9696-z.
- Martínez Oliveros, J.-C., Hudson, H.S., Hurford, G.J., Krucker, S., Lin, R.P., Lindsey, C., Couvidat, S., Schou, J., Thompson, W.T.: 2012, The Height of a White-light Flare and Its Hard X-Ray Sources. *Astrophys. J. Lett.* **753**, L26. doi:10.1088/2041-8205/753/2/L26.
- Maurya, R.A., Ambastha, A.: 2010, A Technique for Automated Determination of Flare Ribbon Separation and Energy Release. *Solar Phys.* **262**, 337–353. doi:10.1007/s11207-009-9488-5.
- Maurya, R.A., Vemareddy, P., Ambastha, A.: 2012, Velocity and Magnetic Transients Driven by the X2.2 White-light Flare of 2011 February 15 in NOAA 11158. *Astrophys. J.* **747**, 134. doi:10.1088/0004-637X/747/2/134.
- Moradi, H., Donea, A.-C., Lindsey, C., Besliu-Ionescu, D., Cally, P.S.: 2007, Helioseismic analysis of the solar flare-induced sunquake of 2005 January 15. *Mon. Not. Roy. Astron. Soc.* **374**, 1155–1163. doi:10.1111/j.1365-2966.2006.11234.x.
- Neidig, D.F.: 1986, On the possibility of a purely chromospheric origin for the bright kernels in white light flares. In: D. F. Neidig (ed.) *The lower atmosphere of solar flares; Proceedings of the Solar Maximum Mission Symposium*, National Solar Observatory 142–151.
- Norton, A.A., Graham, J.P., Ulrich, R.K., Schou, J., Tomczyk, S., Liu, Y., Lites, B.W., López Ariste, A., Bush, R.I., Socas-Navarro, H., Scherrer, P.H.: 2006, Spectral Line Selection for HMI: A Comparison of Fe I 6173 Å and Ni I 6768 Å. *Solar Phys.* **239**, 69–91. doi:10.1007/s11207-006-0279-y.
- Qiu, J., Gary, D.E.: 2003, Flare-related Magnetic Anomaly with a Sign Reversal. *Astrophys. J.* **599**, 615–625. doi:10.1086/379146.
- Qiu, J., Lee, J., Gary, D.E., Wang, H.: 2002, Motion of Flare Footpoint Emission and Inferred Electric Field in Reconnecting Current Sheets. *Astrophys. J.* **565**, 1335–1347. doi:10.1086/324706.
- Rajaguru, S.P., Hughes, S.J., Thompson, M.J.: 2004, Comparison Of Noise Properties Of GONG And MDI Time-Distance Helioseismic Data. *Solar Phys.* **220**, 381–398. doi:10.1023/B:SOLA.0000031396.28529.2e.
- Rust, D.M., Hegwer, F.: 1975, Analysis of the August 7, 1972 white light flare - Light curves and correlation with hard X-rays. *Solar Phys.* **40**, 141–157. doi:10.1007/BF00183158.
- Schou, J., Scherrer, P.H., Bush, R.I., Wachter, R., Couvidat, S., Rabello-Soares, M.C., Bogart, R.S., Hoeksema, J.T., Liu, Y., Duvall, T.L., Akin, D.J., Allard, B.A., Miles, J.W., Rairden, R., Shine, R.A., Tarbell, T.D., Title, A.M., Wolfson, C.J., Elmore, D.F., Norton, A.A., Tomczyk, S.: 2012, Design and Ground Calibration of the Helioseismic and Magnetic Imager (HMI) Instrument on the Solar Dynamics Observatory (SDO). *Solar Phys.* **275**, 229–259. doi:10.1007/s11207-011-9842-2.
- Shih, A.Y., Lin, R.P., Smith, D.M.: 2009, RHESSI Observations of the Proportional Acceleration of Relativistic >0.3 MeV Electrons and >30 MeV Protons in Solar Flares. *Astrophys. J. Lett.* **698**, L152–L157. doi:10.1088/0004-637X/698/2/L152.

- Toner, C.G., Labonte, B.J.: 1993, Direct Mapping of Solar Acoustic Power. *Astrophys. J.* **415**, 847–851. doi:10.1086/173206.
- Švestka, Z.: 1970, The Phase of Particle Acceleration in the Flare Development. *Solar Phys.* **13**, 471–489. doi:10.1007/BF00153567.
- Xu, Y., Cao, W., Liu, C., Yang, G., Qiu, J., Jing, J., Denker, C., Wang, H.: 2004, Near-Infrared Observations at 1.56 Microns of the 2003 October 29 X10 White-Light Flare. *Astrophys. J. Lett.* **607**, L131–L134. doi:10.1086/422099.
- Zharkov, S., Zharkova, V.V., Matthews, S.A.: 2011, Comparison of Seismic Signatures of Flares Obtained by SOHO/Michelson Doppler Imager and GONG Instruments. *Astrophys. J.* **739**, 70. doi:10.1088/0004-637X/739/2/70.